ELSEVIER

Surface Science 492 (2001) 329–344

SURFACE SCIENCE

www.elsevier.com/locate/susc

First-principles calculations for V_xO_y grown on Pd(1 1 1)

G. Kresse [a,*], S. Surnev [b], M.G. Ramsey [b], F.P. Netzer [b]

[a] *Institut für Materialphysik, Universität Wien and Center for Computational Materials Science, Sensengasse 8/12, A-1090 Wien, Austria*
[b] *Institut für Experimentalphysik, Karl-Franzens-Universität Graz, A-8010 Graz, Austria*

Received 17 January 2001; accepted for publication 17 July 2001

Abstract

An approach to access the stability of oxides growing on top of a metal support is presented. In combination with first-principles calculations, it allows to predict the stable structures as a function of the thickness of the evaporated metal ad-layer and as a function of the oxygen pressure. The ideas are applied to thin vanadium oxide films growing on Pd(1 1 1). To investigate the stability of these oxide films, first-principles calculations for more than 50 thin films of V_xO_y on Pd were performed at varying stoichiometry and coverage. The general principles determining the growth of thin vanadium oxide films on Pd(1 1 1) are discussed, and the experimental results are interpreted in the light of the first-principles calculations. At 1 ML vanadium coverage, a complicated succession of structures is predicted by the calculations. At high oxygen pressure bulk like V_2O_3 phases are stable. At lower oxygen pressure, however, a surface stabilised (2×2) reconstruction with a formal stoichiometry of V_2O_3 is predicted, and rectangular and hexagonal vanadium-dioxide phases are expected to grow. At very low oxygen pressures, first the vanadium-dioxide phases and then the surface V_2O_3 phase decompose and the liberated V atoms move subsurface. These predictions are in good general agreement with experiment. An important result of the study is that the metal surface stabilises thin films which have no equivalent bulk phases.

Keywords: Density functional calculations; Equilibrium thermodynamics and statistical mechanics; Growth; Vanadium oxide; Palladium; Metal–semiconductor interfaces

1. Introduction

The growth of thin oxide films on a metal support is a fascinating field of surface science which has recently gained substantial attention. The interest partly stems from the technological importance of thin oxide films, but also from a fundamental point of view these materials are a challenge. It is unclear to which extent the physical, chemical and structural properties of thin films differ from those of bulk materials, and how growth and morphology are affected by the metal support [1–4]. The experimental characterisation of such films has become possible with modern surface science methods, but even if a large variety of experimental data exists, precise atomistic structural models remain difficult to construct. With their predictive power, first-principles calculations are obviously an ideal supplement to the experimental techniques, but their application to such complex systems is still in their infancy.

* Corresponding author. Tel.: +43-1-4227-51402; fax: +43-1-4277-9514.
E-mail address: georg.kresse@univie.ac.at (G. Kresse).

0039-6028/01/$ - see front matter
PII: S0039-6028(01)01454-6

In the work presented here the materials under study are thin films of vanadium oxide on Pd(1 1 1). The growth of vanadium oxides on metal surfaces is currently an active field driven by the need to prepare well characterised vanadium oxide films of varying stoichiometry. The properties of such films can then be studied with surface sensitive techniques that would usually be only applicable to metallic surfaces. For our first-principles study we have chosen Pd as support, since a considerable amount of data has accumulated in recent years for thin films of vanadium oxides grown on Pd(1 1 1), including core-level spectra [5], scanning tunnelling microscopy (STM) images [5–7], high resolution electron energy loss spectroscopy (HR-EELS) [8], and near-edge X-ray absorption fine structure (NEXAFS) data [5]. Despite the wealth of information, it turned out to be difficult to derive atomistic models for most of the observed phases. Part of the problems are related to the fact that vanadium can occur in various oxidation states ranging from V^{2+} (VO) to V^{5+} (V_2O_5), and unfortunately the stoichiometry is difficult do determine from V core-level spectra alone, since the core levels are significantly affected by the metallic substrate. On the other hand, the experimental data allow to narrow the structures one has to investigate in first-principles calculations. For instance, (2×2) STM images and LEED patterns were observed under a variety of experimental conditions. Even though the stoichiometry could not be determined by experiments alone, it was fairly straightforward to construct a number of plausible atomistic models, to test their local stability with first-principles methods, and to compare experimental and theoretical vibrational frequencies and STM images. In our recent work, we established in this way that the available experimental data for the (2×2) superstructure can be reconciled with a novel s-V_2O_3 phase which has no equivalent in the bulk [6].

Here, our aims are somewhat more ambitious: we want to determine the stable structures for varying stoichiometries and coverage by means of the *energies* predicted by first-principles calculations. To construct the required phase stability diagram, we need to explore a large number of stoichiometries and reconstructions. Of course such calculations necessarily face limitations, since the investigations must be restricted to a selected number of superstructures. Here, we have limited our calculations to $(\sqrt{3} \times \sqrt{3})$ and (2×2) supercells, where reconstructions with a periodicity of (1×1) and (2×1) are also implicitly covered. Significantly larger systems are difficult to treat, since also a large number of models must be considered at a specific stoichiometry and periodicity. On the other hand, the experiments seem to justify our choice, because with one exception no long range ordered superstructure was observed experimentally. The exception is a VO_2 phase [7], which seems to be incommensurable with the Pd(1 1 1) substrate, also implying that the phase cannot be studied in a straightforward manner in a super cell calculation. To assert the stability of such incommensurable phases we will also present results on thin unsupported vanadium oxide films.

Even with the restriction to $(\sqrt{3} \times \sqrt{3})$ and (2×2) superstructures, the number of explored models remains large. In some cases, symmetry arguments and/or chemical intuition can help to restrict the choices further, but intuition is often prone to failure. To be less biased simulated annealing runs were often performed to establish that the investigated structures are indeed global energy minima. In total, more than 50 models were constructed and tested in the course of this work, but we will necessarily restrict the discussion mainly to more favourable configurations. We will show that three very different categories of oxides are stable on the surface. The first category is similar to bulk like V_2O_3 (corundum), with an oxygen termination at the vacuum and an oxygen layer at the interface. The second class of oxides are thin rectangular or hexagonal vanadium-dioxide films, which interact only weakly with the substrate. Finally, one surface stabilised phase exits (s-V_2O_3), which was already investigated in some detail in Ref. [6].

The paper is organised in the following way. We will first briefly discuss the methods used in the present work (Section 2). Then results for bulk vanadium oxides (Section 3.1) and for unsupported oxide films are presented (Section 3.2). The insight gained from these calculations is used to construct models for thin supported oxide films (Sections 3.4–3.7), and the general principles which

govern the stability of thin vanadium oxide films on Pd(1 1 1) are discussed in Section 4.2. In Section 4.1 our results are confronted with the experimental data.

2. Methodology

2.1. First-principles calculation

Our first-principles calculations are based on density-functional theory (see eg. Refs. [9,10]) and employ a plane wave basis set [11,12]. As in our previous work (see Ref. [6]) we use the Vienna ab-initio simulation package (VASP) [13–15], where in the most recent version the interaction between the ions and electrons is described by the projector augmented wave (PAW) [16] method in the implementation of Kresse and Joubert [17]. The technical parameters are identical to Ref. [6]: the Pd surface is modelled by a four layer Pd slab (two layers are allowed to relax), and the lattice constant is fixed to the theoretical Pd fcc lattice constant ($a_{\text{theory}} = 3.95$ Å, $a_{\text{exp}} = 3.89$ Å). The generalised gradient approximations (GGA) of Perdew and Wang [18,19], commonly referred to as PW91, are used throughout this work.

To sample the band-structure a grid corresponding to $8 \times 8 \times 1$ k-points in the primitive surface cell is chosen. For a (2×2) supercell this corresponds to $4 \times 4 \times 1$ k-points. We did careful tests to ensure that the results are well converged with respect to the slab thickness and with respect to the k-point sampling. When we increased the slab thickness from four to six layers and increased the k-point grid to $6 \times 6 \times 1$ points for the (2×2) s-V_2O_3 model (see Ref. [6]), the adsorption energies changed by less than 15 meV. Hence, we expect that the average errors in the reported energies are about 20 meV, which is sufficient for the present purpose.

2.2. Energy stability of explored models

To characterise the stability of the explored models, we use a generalised adsorption energy E_{ad} defined as

$$E_{\text{ad}} = E_{\text{V}_x\text{O}_y/\text{slab}} - (E_{\text{slab}} \pm N_{\text{Pd}}\mu_{\text{Pd}}) - N_{\text{V}}\mu_{\text{V}} - N_{\text{O}}\mu_{\text{O}}. \quad (1)$$

$E_{\text{V}_x\text{O}_y/\text{slab}}$ and E_{slab} are the energies of the explored model and the clean Pd-slab, respectively. The models allow for a replacement of surface or subsurface Pd atoms by V atoms, or the addition of Pd atoms to the surface, and the number of Pd atoms removed or added to the slab is denoted by N_{Pd}. We must allow for such processes, since Pd atoms are available on the surface by evaporation from steps. In equilibrium, the chemical potential of a Pd atom is given by $\mu_{\text{Pd}} = E_{\text{Pd}}(\text{fcc})$, since – in simple terms – the *average* energy for removal of a step atom equals the energy of an atom in the bulk. With respect to Pd, the grand-canonical potential is effectively considered assuming equilibrium between the surface and the bulk. The reference energy for V, μ_{V}, is set to the energy of a bcc bulk V atom, and μ_{O} is set to half of the energy of an oxygen dimer. These two values define the energy zero for O and V, but we will discuss below that results do not depend on the precise reference values.

To establish the stability of a particular structure we first calculate the average energy of formation per ad-atom

$$E_{\text{form}} = \frac{E_{\text{ad}}}{N_{\text{V}} + N_{\text{O}}}, \quad (2)$$

and plot this value against the concentration of V atoms

$$x_{\text{V}} = \frac{N_{\text{V}}}{N_{\text{V}} + N_{\text{O}}}. \quad (3)$$

As will be shown at the end of this paragraph, this quantity can be used to asses the stability of a particular structure as long as part of the Pd surface is *not* covered by any adsorbate (free surface area is accessible). In this case, stable structures are those which lie on a concave curve, as illustrated in Fig. 1. This is similar to the construction of the phase diagram of a binary alloy, and to show that this description is correct, we resort to the usual arguments based on the surface energy. The most stable structure will result in the lowest surface energy, and it is easy to see that adsorption

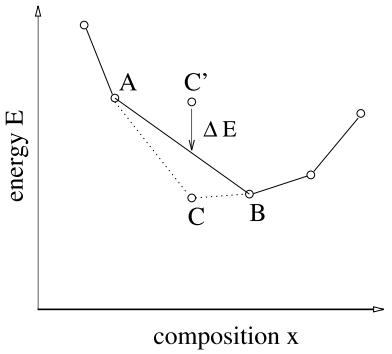

Fig. 1. Schematic energy–composition diagram. The structure C′ is unstable and will decompose into structures A and B with an energy gain of ΔE per atom. Structure C is stable. Generally only phase points that lie below lines connecting any other two points are stable, and the resulting curve is always concave.

of an oxide in the structures A, B and C decreases the total surface energy by $\Delta E^X_{\text{surf}} = N_X E^X_{\text{form}}$, where N_X is the total number of adsorbed atoms. Exactly the same quantity, $N_X E^X_{\text{form}}$, determines the stability of binary alloys, which immediately shows the validity of the previous argument. The second important point is that a redefinition of the reference energies of oxygen, μ_{O}, or vanadium, μ_{V}, will redefine only the slopes of all lines, but the stability considerations will not be affected. We stress again, that this approach works only in the low coverage limit, since it assumes that phases can freely decompose into other phases consuming free surface area.

To discuss the case when the whole Pd surface is covered with an oxide, we have to use an alternate description. We define the change in the surface energy per surface area as

$$\Delta E_{\text{surf}} = \frac{E_{\text{ad}}}{n_{\text{cell}}}, \tag{4}$$

where n_{cell}, is the number of primitive surface cells in the slab model. Similar to the previous case the chemical potential of Pd is set to $\mu_{\text{Pd}} = E_{\text{Pd}}(\text{fcc})$, which simply assumes that the surface is in equilibrium with bulk Pd. The chemical potential of vanadium, μ_{V}, is again set to $E_{\text{V}}(\text{bcc})$, but the final results will not depend on this choice. The chemical potential of oxygen, μ_{O}, is now treated as an extrinsic thermodynamic variable, which is supposed to be determined by the experimental setup. Then we plot the change in the generalised surface energy, ΔE_{surf}, for each structure versus the nominal V coverage of this structure for a set of μ_{O} (for more details see Section 4.1). Along similar arguments as before, it can be shown that stable phases must lie again on a concave curve (compare again Fig. 1), but now the oxygen potential is an extensive (externally controlled) degree of freedom. On the other hand, a redefinition of the chemical potential of V will again only change the slope of all lines by the same value, so that the stability considerations are not affected by such a change. The approach taken here is similar in spirit to the stability considerations of surfaces of compounds [20–23] but complicated by the fact that we have to consider three constituents instead of two. In addition, we transform to the grand-canonical potential only with respect to oxygen and treat the V coverage as the second extensive thermodynamic variable. This description was chosen, since it corresponds to the experimental setup in which the V coverage and the oxygen partial pressure are controlled [5,6].

3. Results

3.1. V_xO_y bulk phases and convergence tests

To check the accuracy of the setup, first-principles calculations for four bulk vanadium oxide phases and oxygen chemisorbed on Pd(1 1 1) were performed, paying particular attention to the oxygen potential and the energy cutoff. Further results, in particular results for low symmetry and low temperature V_xO_y phases and a discussion of electronic properties will be published elsewhere, since this is beyond the scope of the present work [24].

Table 1 summarises the lattice constants of the considered oxides and compares them with experimental data. The heat of formation with respect to bulk V and the O_2 dimer are shown in Fig. 2. All bulk calculations and the surface calculations reported in the later sections were performed with a rather "soft" oxygen potential at an

Table 1
Lattice constants of bulk vanadium and vanadium oxides considered in the present work. Also shown is the bond length of the oxygen dimer (all values in Å)

Comp.	Type	Experiment	Theory
O_2	Dimer	$a = 1.21$	$a = 1.22$
V_2O_5		$a = 11.51$,	$a = 11.65$,
		$b = 3.57$,	$b = 3.57$,
		$c = 4.37$[a]	$c = 4.69$
VO_2	Rutile	$a = 4.55$,	$a = 4.61$,
		$c = 2.85$[b]	$c = 2.80$
V_2O_3	Corund. RAF	$a = 4.94$,	$a = 4.90$,
		$c = 13.97$[c]	$c = 14.25$
VO	NaCl	$a = 4.07$[d]	$a = 4.19$
	Vacancy		$a = 3.93$
V	bcc	$a = 3.03$	$a = 2.99$

RAF refers to the anti-ferromagnetic ordering described in Ref. [33].
[a] Ref. [25].
[b] Ref. [28].
[c] Ref. [29].
[d] Ref. [34].

energy cutoff of 250 eV. During the relaxation of the bulk phases the lattice parameters and the positions were allowed to change, and the energy cutoff was increased to avoid problems with basis set incompleteness errors. Since the soft oxygen potential is not able to describe molecules with short O–O bond-length, the reference energy for the O_2 dimer was calculated with a hard and accurate oxygen potential (500 eV energy cutoff).

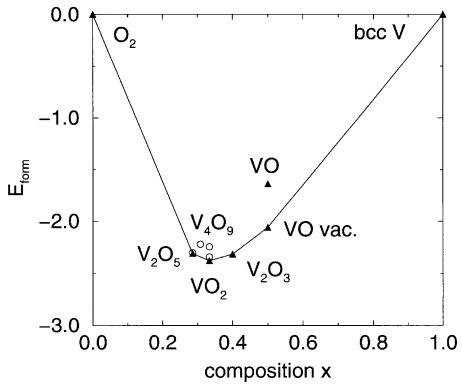

Fig. 2. Formation energy of bulk and film vanadium oxides. Filled triangles correspond to bulk phases, circles to thin film-phases (see text). The two circles at the stoichiometry VO_2 correspond to the hexagonal (upper circle) and the rectangular (lower circle) VO_2 film.

The oxygen richest compound is V_2O_5, which forms a layered structure and is an insulator. Our final structural data agree well with the experimental data [25] and to a lesser extent with previous theoretical calculations (in Refs. [26,27], the local density approximation was used leading to an underestimation of all lattice parameters). Only the distance between the V_2O_5 layers is significantly overestimated, which we attribute to the fact that gradient corrected functionals do not account very accurately for Van der Waals bonding.

VO_2 [28] and V_2O_3 [29] were considered only in the metallic high temperature phases (rutile and corundum structure respectively) and we find for both structures reasonable agreement with experiment. The low temperature phases are Mott-Hubbard insulators [30], for which present density functionals fail to work satisfactory [31–33].

Bulk VO [34] was initially investigated in the NaCl structure, for which the lattice constant is significantly overestimated compared to experiment. In addition, Fig. 2 shows that VO decomposes into V and V_2O_3. If 25% vanadium and 25% oxygen vacancies are introduced by removing one V atom and one O atom from the the edge and the centre of a V_4O_4 cube, VO becomes stable (a similar vacancy structure was reported for NbO) [35]. In this case, the lattice constant is smaller than in the experiment, which could be attributed to disorder or to a reduced vacancy concentration in real VO.

As an additional test, the adsorption energy of atomic oxygen on Pd(1 1 1) in the p(2 × 2) structure was calculated. We found a value of 1.36 eV with respect to half an O_2 dimer. Careful tests for oxygen adsorption on Pd(1 1 1) and for several vanadium oxide structures with a harder and more accurate oxygen potential at an energy cutoffs of 500 eV indicate that all calculated energies are accurate to within 20 meV, which we consider to be sufficient for the present purpose.

In passing, we want to point out that for an oxidation state between +III and +V, vanadium atoms typically prefer an octahedral environment. VO, corundum V_2O_3, rutile VO_2 and even V_2O_5

can be build by a proper arrangement of such octahedrons. The V–O bond-length increases from 1.91 Å in VO_2, over 1.97 Å in V_2O_3 to 2.09 Å in VO. One can expect that such building units will remain relevant in thin films and thin films grown on the Pd(1 1 1) surface.

3.2. Thin unsupported layers

Before considering vanadium oxides grown on Pd(1 1 1), we will briefly discuss the stability of few thin unsupported oxide layers. These calculations are partly motivated by the fact that an incommensurable oxide layer was observed to grow on Pd(1 1 1) under certain experimental conditions (VO_2 phase, see Refs. [5,7]). Since the interaction of such a layer with the substrate is weak, it seems reasonable to model such a layer without the Pd support. Secondly, results for thin unsupported layers are helpful for the construction of compact oxide layers which are commensurable with the Pd(1 1 1) surface, and many of the oxides considered in later sections resemble the thin films discussed below.

One way to construct such thin layers is by cleaving vanadium oxides along low index symmetry planes. If one follows this route for oxygen rich oxides – like VO_2 or V_2O_3 – and cleaves in a way that leaves the stoichiometry conserved, the octahedral environment of V atoms is strongly disturbed, and such models are generally not particularly favourable. If, on the other hand, all O–V bonds around V atoms are left intact, unreasonable V oxidation numbers are often obtained also leading to instabilities. This problem can be surmounted by cleaving e.g. VO so that the octahedral environment around V atoms is left intact.

We start with the highest oxidation number of vanadium corresponding to V_2O_5. Since V_2O_5 is a layered structure and since the interaction between the layers is known to be weak [26,27], a single V_2O_5 layer is very stable. We found a formation energy of $E_{\mathrm{form}} = -2.30$, which is only some 10 meV less than for bulk-V_2O_5.

For V_4O_9, bulk-V_2O_3 was cleaved parallel to two basal planes, leaving three O_3 and two V_2 planes with a stacking sequence of $O_3V_2O_3V_2O_3$. Thinner layers are unfavourable, since the oxidation number of V becomes either unreasonable or the vanadium coordination is disturbed significantly, as discussed before. The formation energy of the V_4O_9 model is −2.22 eV, and the substrate supported case of this structure is shown in Fig. 3(c). The structure shows only negligible spin polarisation in contrast to the bulk-V_2O_3 phase.

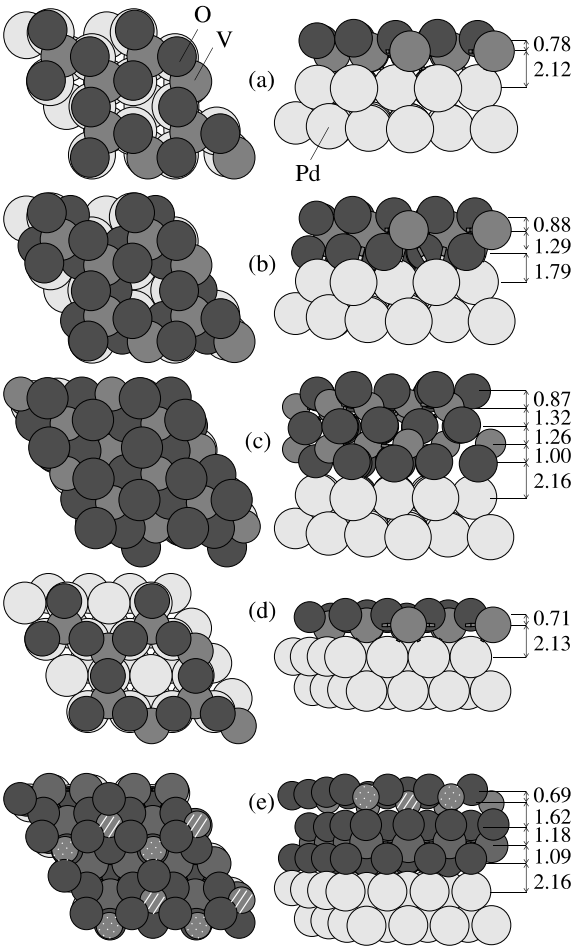

Fig. 3. Structures discussed in this work. Supercells with $(\sqrt{3} \times \sqrt{3})$ periodicity: (a) one layer of bulk-like V_2O_3 on Pd(1 1 1) with the vacuum side only oxygen terminated, (b) bulk-like V_2O_3 with both sides oxygen terminated, (c) two layers of bulk-like V_2O_3 on Pd(1 1 1) both sides oxygen termined. Supercells with with (2×2) periodicity: (d) s-V_2O_3 and (e) hexagonal VO_2 with s-V_2O_3 on top. For structure (e) the V atoms in the topmost layer have either an octahedral (dashed) or a tetrahedral (dotted) coordination. The average distance between the layers is indicated on the right (all distances in Å).

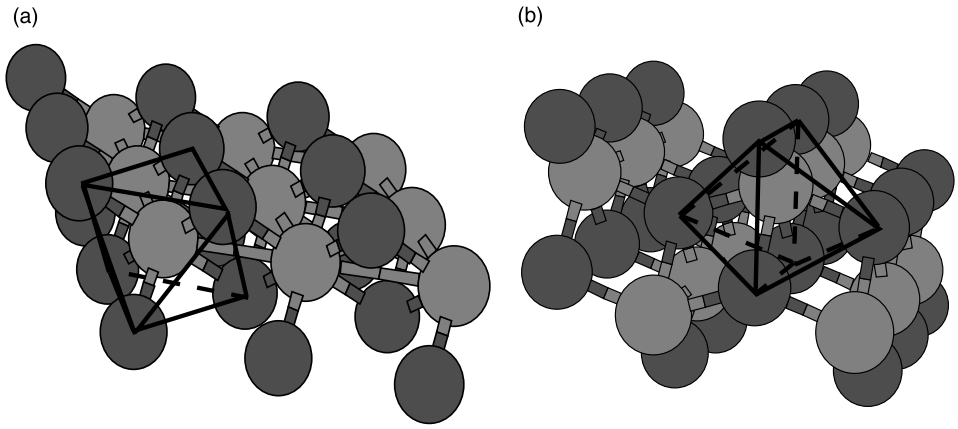

Fig. 4. (a) Hexagonal and (b) rectangular model for thin unsupported VO_2 as obtained by cleaving bulk VO (see text). The V atoms and O atoms are coloured medium grey and dark grey. The basic building units, i.e. VO_6 octahedrons, are also shown.

At the stoichiometry VO_2, three models were considered, all obtained by cleaving bulk VO. In the first case, VO was cleaved along two (1 1 1) planes leading to a hexagonal layer of V atoms and two also hexagonal oxygen layers above and below the V atoms (see Fig. 4(a)). Initially, the lattice constant of such a model is $a = 3.62$ Å, but structural relaxation to the groundstate leads to a reduction of the lattice constant to $a = 2.87$ Å, which is close to that of the Pd(1 1 1) surface. The height of the model is 2.04 Å (oxygen core–core distance). The formation energy is $E_{\text{form}} = -2.25$ eV, and each V atom has a magnetic moment of $1\mu_B$.

Cleavage along the (1 1 0) plane of VO is somewhat more complicated, since in the (1 1 0) direction a plane contains the same number of vanadium and oxygen atoms. We keep two adjacent vanadium oxide planes and add from two additional planes the oxygen atoms only, so that the octahedral coordination of vanadium atoms is maintained. The final structure is visualised in Fig. 4(b). The initial lattice constants are $a = 2.88$ Å and $b = 4.07$ Å and relax to $a = 2.96$ Å and $b = 3.71$ Å. The height of the model is 4.2 Å. With a formation energy of -2.34 eV, this structure is more stable than the previous hexagonal model, and, as will be discussed in Section 4.1, the lattice parameters agree well with the thin VO_2 phase of Ref. [7]. In the rest of this work, we will refer to this model as rectangular VO_2 film. The magnetic moment of each vanadium atom is again $1\mu_B$.

Finally, cleavage along the (1 0 0) plane of VO was considered. Again two adjacent vanadium oxide planes were kept, and the oxygen atoms of two additional layers added on the top and bottom in a way that leaves the local coordination of V atoms intact. It turns out that this is the most unfavourable cleavage plane for VO, and the formation energy is only -2.08 eV.

Further reduced oxide layers were not considered, since the octahedral coordination of V atoms would be significantly disturbed in these cases. Generally such models are found to be rather unfavourable. The energies of the thin films discussed until now are compared to the formation energies of bulk phases in Fig. 2.

3.3. Simulated annealing run for a (4×4) stepped surface

To gain insight which structures are preferred by vanadium oxides on the Pd surface in the low coverage case, we performed a short finite temperature molecular dynamics (MD) simulation. The Pd surface was modelled by a stepped (4×4) supercell. Only three layers were included in the

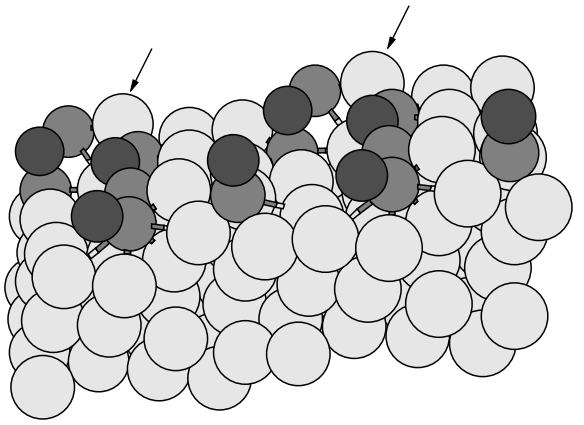

Fig. 5. Final structure obtained in a simulated annealing run for V_6O_4 on a stepped (4×4) Pd(1 1 1) surface. Two unit cells are shown. The Pd atoms are coloured light gray, the V atoms are medium grey, and the O atoms are dark grey.

calculation, and the bottom layer was kept fixed during the MD simulation. Six vanadium and four oxygen atoms were placed on the surface, all initially occupying hollow sites. The temperature during the simulation was set to 1200 K and gradually decreased to 300 K. Since the total simulation time was relatively short (4 ps), we cannot expect to find the real zero temperature equilibrium groundstate but hope to get some indication for the preferred positions of V and O atoms.

The final structure for the V_6O_4/Pd MD simulation is shown in Fig 5. One V atom has replaced a surface Pd atom which has in turn diffused to the step (arrows in Fig. 5). A second V atom occupies a three fold hollow site, and the remaining four V atoms have attached to the step. Three of the oxygen atoms are bridge bonded between two V atoms. The remaining fourth oxygen atom is coordinated to the V atom in the hollow site.

The results can be rationalised in the following way. First, a strong tendency towards V–Pd hetero-coordination exists. This is also confirmed in first-principles calculations for the adsorption of V on Pd (see Ref. [36]). Here we want to summarise only the most important results of these calculations. In the V–Pd surface alloy, V atoms try to maximise their coordination to Pd atoms. V atoms *on* the surface prefer the hollow sites but are unstable towards diffusion into the surface or bulk. If a V atom replaces a surface atom, it gains an energy of $E_{\text{form}} = -0.8$ eV, and V atoms in subsurface sites or the formation of a dilute V–Pd bulk alloy yields an energy gain of the order of $E_{\text{form}} = -1.8$ eV per V atom. The MD simulation presented here shows that the trend towards V–Pd hetero-coordination prevails in the case of oxidised V atoms: V atoms prefer positions in which the coordination to Pd atoms is large (substitutional surface sites, step edges and hollow sites). Our MD also clearly shows that the oxygen atoms tend to bind to V atoms and not to surface Pd atoms. This is an indication for the strong reactivity of V. In addition, the oxygen atoms are preferentially bonded to more than one V atom, and the bridge bonded position between two V atoms is particularly favourable.

3.4. General strategies for the construction of surface models

With the calculations presented so far we are armed with the required insight to build more complex models for vanadium oxides on Pd(1 1 1). For "compact" layers, i.e. a V-coverage exceeding about 1/2 ML, one can expect similar structures as for bulk or thin unsupported vanadium oxide layers, whereas for small V concentrations the results of the MD should prove useful: V atoms prefer sites in which the Pd coordination is maximised, and oxygen atoms are preferentially bridge bonded. In the construction of starting models, we have therefore adopted three different strategies: (i) For compact over-layers, the starting models are similar to the thin film phases discussed in Section 3.2. Only two structures are commensurable with the hexagonal Pd(1 1 1) surface. These are bulk-V_2O_3 (and the corresponding thin films) and the hexagonal thin VO_2 film. Even with this restriction, a large number of different stacking sequences has to be explored. (ii) For small vanadium coverage one must proceed along a different line. It turns out that the most successful strategy is to place vanadium atoms at their preferred sites (Pd-surface sites, hcp and fcc hollow sites) and to

add oxygen atoms in a way that they are bonded to at least two V atoms. Since the oxygen–vanadium bond length is typically around 1.8 Å, sensible distances between two vanadium atoms range from 2.8 to 3.6 Å. This leaves only very few useful configurations: for instance, two vanadium atoms in two neighbouring fcc (hcp) hollow sites, or one V in a hcp and the second one in the second nearest fcc site. If V atoms occupy surface sites, oxygen can only coordinate to two V atoms, if the V atoms occupy neighbouring surface sites. (iii) Finally, in some cases, simulated annealing runs were used either to get new structural models or to confirm the global stability of one particular model.

The energies of the most relevant phases are summarised in Table 2, and the energies of the important low coverage phases are shown in Fig. 6. On the left-hand side of the energy diagram (oxygen rich case), the most stable phase is the oxygen $p(2 \times 2)$ phase, where oxygen atoms are adsorbed in fcc hollow sites at 1/4 ML. With respect to an oxygen dimer, the energy gain upon adsorption is 1.36 eV per oxygen atom.

On the right-hand side of the diagram (no oxygen), the largest energy amount can be gained by diffusion of V atoms into the Pd bulk. In this case, each V atom gains 1.81 eV [36]. For the migration of V into the bulk, barriers must be overcome and depending on the experimental preparation this configuration might not be always accessible [36]. If the diffusion of V to the bulk is in some

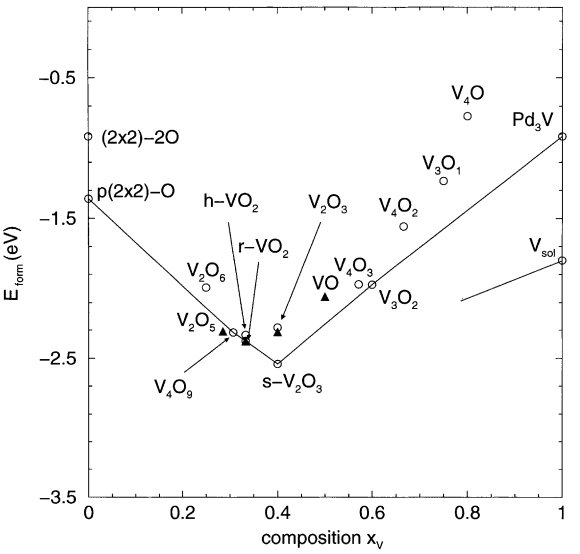

Fig. 6. Formation energy E_{form} versus composition x for vanadium oxides on Pd(1 1 1) (structural models are discussed in the text). For comparison, the bulk formation energies of V_2O_5, VO_2, V_2O_3 and VO are shown as filled triangles. Table 2 summarises the relevant phases.

Table 2
Definition of the shortcuts for the structures discussed in this work. Also shown is the nominal V coverage for each structure, where a coverage of 1 ML corresponds to 1 V atom per primitive surface unit cell. The formation energies E_{form} are reported for the substrate supported case

Shortcut	V-coverage (ML)	E_{form} (eV)	Description
$p(2 \times 2)$-O	0	−1.360	O adsorbed in the $p(2 \times 2)$ structure
V_2O_5	0.659	−2.300	Single layer of bulk-V_2O_5
V_2O_3	2/3	−2.281	One layer of bulk-V_2O_3, vacuum side O-terminated (Fig. 3(a))
V_4O_6	4/3	−2.184	Two layers of bulk-V_2O_3, vacuum side O-terminated
V_6O_9	6/3	−2.232	Three layers of bulk-V_2O_3, vacuum side O-terminated
V_2O_6	2/3	−1.992	One layer of bulk-V_2O_3, both sides O-terminated (Fig. 3(b))
V_4O_9	4/3	−2.316	Two layers of bulk-V_2O_3, both sides O-terminated (Fig. 3(c))
V_6O_{12}	6/3	−2.334	Three layers of bulk-V_2O_3, both sides O-terminated
r-VO_2	1.23	−2.376	Thin rectangular layer (see Fig. 4(b))
h-VO_2	1	−2.335	Thin hexagonal layer (see Fig. 4(a))
s-V_2O_3	1/2	−2.540	S-V_2O_3 (Fig. 3(d))
V_6O_{11}	1.5	−2.376	(2×2) h-VO_2 plus an overlayer of s-V_2O_3 (see Fig. 3(e))
$V_4O_{1,2,3}$	1		A monolayer of V, with O adsorbed in hollow sites
$V_3O_{1,2}$	3/4		Three V atoms replacing Pd surf.-atoms, O adsorbed in hollow sites
V_{sol}	Any	−1.8	V forming a solid solution in fcc Pd

way hindered, another plausible configuration is a surface alloy with a stoichiometry of Pd_3V. The most stable bulk structure at this stoichiometry is the Al_3Ti structure with a formation energy of -0.915 eV per V-atom. Similar values are found for simple surface alloys in which every fourth Pd surface atom is replaced by a V atom [36].

In the following sections, we will discuss the results at different stoichiometries in more detail. The discussion will first focus on the bulk-V_2O_3 derived structures and the V_2O_3 stoichiometry, since particularly stable configurations can be observed in these cases. Then we will focus on the oxygen rich regime and finally on the (less interesting) vanadium rich regime. A description of the investigated phases is summarised in Table 2.'

3.5. Phases derived from bulk-V_2O_3

Experiments show that bulk-like V_2O_3 grows epitaxially on the Pd(1 1 1) surface. A consideration of the lattice constants of V_2O_3 (experiment $a = 4.91$ Å, theory $a = 4.90$ Å) shows that this fits well with the lattice constant of the $(\sqrt{3} \times \sqrt{3})$ Pd(1 1 1) surface (experiment $a = 4.764$ Å, theory $a = 4.842$ Å) supporting the experimental findings. To study this case, one, two and three layers of bulk-V_2O_3 on Pd(1 1 1) were explored. We considered stackings with oxygen and vanadium at the interface and different terminations at the vacuum side. In general, our calculations clearly indicate that oxygen is located at the metal–oxide interface and the vacuum side at the relevant chemical potentials of oxygen. For thin layers, this causes an increase in the oxygen content V_2O_{3+x} compared to bulk-V_2O_3.

Let us, nevertheless, start with one and two layers of stoichiometric bulk-V_2O_3. The most favourable stacking sequences are Pd–V_2–O_3 (one layer) and Pd–V_2–O_3–V_2–O_3 (two layers), where the V atoms are located in the hcp sites and O atoms are situated atop Pd sites (see Fig. 3(a)). For a single layer of vanadium oxide the formation energy is $E_{\text{form}} = -2.28$ eV and it decreases to $E_{\text{form}} = -2.18$ eV for the double layer. Both values are smaller than the bulk values ($E_{\text{form}} = -2.32$ eV), which we attribute to finite size effects (formation of the surface and the interface). When additional layers are added the energy gain per added layer equals that of bulk-V_2O_3, so that the formation energy of thicker layers converges towards the bulk-V_2O_3 value (e.g. V_6O_9, see Table 2).

For the cases, in which oxygen is located at the interface and the vacuum side, we started our calculations with a single layer corresponding to $O_3V_2O_3$. Formally this corresponds to a stoichiometry of VO_3, which can and does not exist in a bulk-like phase (a thin film of this type is unstable too). But here one oxygen layer is in contact with the Pd surface leading to a covalent bonding between the oxide and the Pd surface (if the film is brought from the vacuum to the Pd-surface, 3.5 eV are gained per V_2O_6 unit). The most favourable stacking sequence is Pd(A)–Pd(B)–Pd(C)–O(A)–V(B)–O(C) (see Fig. 3(b)), where A, B and C are used to label the layers in the fcc crystal. The Pd–O distance is 2.1 Å, which is only slightly larger than the distance between atomic oxygen and Pd, corroborating the existence of a covalent bond between the oxygen layer and the Pd substrate. Among the explored stacking sequences was also one recently proposed by Jennison et al. for $O_3Al_2O_3$ on fcc-Al, in which Al and V, respectively, have a tetragonal coordination (stacking: Pd(A)–Pd(B)–Pd(C)–O(A)–V(A)–O(C)) [37]. We found this model to be less favourable in the present case (100 meV/atom), which relates to the fact that the tetragonal coordination is not favoured by V in any oxidation state.

The stability is much enhanced for two layers bulk-V_2O_3 ($O_3V_2O_3V_2O_3$), corresponding to a stoichiometry of V_4O_9 (compare Fig. 3(c)). As a result of the reduced oxygen concentration, the bonding to the substrate is much weaker and the distance of the ad-layer is larger than for a single layer. The weaker substrate binding is also reflected by the energy gain for bringing the oxide from the vacuum to the surface which is now only 1.3 eV (440 meV for each O–Pd bond). Also the most stable stacking sequence is different, and the oxygen atoms are now situated above the Pd sites (the typical Pd–O bond length is again some 2.1 Å). The results for three layers can be found in Table 2 (V_6O_{12}).

3.6. Surface stabilised phases

With the restriction to (2×2) and $(\sqrt{3} \times \sqrt{3})$ models, we have to consider only one additional case for the stoichiometry V_2O_3: V_2O_3 in a (2×2) supercell. The most stable structural model is shown in Fig. 3(d). The V atoms now adsorb in a honeycomb pattern (fcc and hcp sites) and O binds to the V–V bridge sites. For this structure the formation-energy ($E_{\text{form}} = -2.54$ eV) is larger than for bulk-like V_2O_3, and we will refer to the model in the following as s-V_2O_3 (surface-V_2O_3). For s-V_2O_3 and a single bulk-like V_2O_3 layer, the O–V bond length at the vacuum side is 1.77 Å. For s-V_2O_3, the oxygen atoms are located exactly at V–V bridge sites, whereas they are moved off bridge for bulk-like V_2O_3, forming an almost ideal hexagonal layer (Fig. 3(a)). The reason for the increased stability of s-V_2O_3, compared to bulk-V_2O_3, is most likely electrostatics. Since the packing of oxygen atoms is significantly lower for this model (2/3 compared to 1 ML for bulk-like V_2O_3), the mutual repulsion between O^{2-} ions is decreased. It is important to stress that s-V_2O_3 is only stable in this thin-film configuration and even the addition of a second layer is energetically very unfavourable [7].

Before continuing, we mention here that we recently identified the s-V_2O_3 structure to be responsible for the experimentally observed (2×2) LEED pattern and STM images [6]. This identification was also supported by simulated core-level shifts and the comparison of the vibrational frequency of the dipole active mode with HR-EELS.

3.7. Thin film phases

The hexagonal VO_2 thin-film phase (compare Fig. 4(a)) is almost commensurate with the substrate, hence we modelled the pseudo-morphic growth of the layer on Pd. On the surface, we found a formation energy of -2.33 eV, which corresponds to a binding energy of 410 meV per Pd–O bond (compared to the isolated h-VO_2 film). A very similar value was already found for the interface energy of the bulk-V_2O_{3+x} phases in Section 3.5. The local coordination of the oxygen atoms is also similar (O above Pd sites). We have also tried to add an add-layer of s-V_2O_3 on top of this hexagonal thin film, corresponding to 4(h-VO_2)/s-V_2O_3 (V_6O_{11}). As will be seen later, this is a very stable phase at higher V coverage. The stable stacking sequence is shown in Fig. 3(e), where, interestingly, half of the vanadium atoms have a tetrahedral coordination in the topmost layer. Stacking sequences without tetrahedrally coordinated V atoms would require that the topmost oxygen layer were located exactly above the central oxygen layer, which is electrostatically unfavourable.

The rectangular VO_2 model (compare Fig. 4(b)) cannot be modelled with the support. But if we assume a smoothly varying Pd–O energy surface which resembles that for the hexagonal over-layer (410 meV atop, 140 meV in the bridge and 100 meV above hollow), and if we further assume that the oxygen atoms at the substrate–oxide interface are randomly distributed, we obtain a typical substrate–oxide binding energy of

$$1/4 \cdot 400 \text{ meV} + 2/4 \cdot 140 \text{ meV} + 1/4 \cdot 100 \text{ meV} \approx 200 \text{ meV}$$

per oxygen atom in contact with the surface. The average formation energy is then -2.38 eV, more stable than the h-VO_2 film.

At this point, it is also instructive to consider the two bulk phases corresponding to the stoichiometries under consideration. V_2O_5 and thin layers of V_2O_5 are more stable than any of the surface oxides considered here (see Fig. 6). From a thermodynamic point of view, we would expect that V_2O_5 grows on Pd (see also Section 4.1). The growth of such a layer is however likely to be kinetically hindered by the strong corrugation of V_2O_5. Bulk-VO_2 is also fairly stable, and its energy is slightly lower than that of the rectangular phase. But as already discussed in Section 3.2 thin films of bulk-VO_2 are generally not favourable, which makes the formation of a nucleus of VO_2 on Pd(1 1 1) also unlikely.

3.8. VO stoichiometry, and further reduced oxides

In our study, a significant effort was devoted to the investigation of the 1:1 stoichiometry, since initially it was assumed that the experimentally observed (2×2) superstructure corresponds to

this stoichiometry. More than 10 models in a (2×2) supercell were explored at this particular composition, and the number of V and O atoms varied between one and four atoms per (2×2) supercell. The general result of our investigation, however, is that none of these structures are thermodynamically stable. Even the most stable ones will decompose into V forming a solid solution in Pd and s-V_2O_3, with an energy gain of about 200 meV per surface atom.

At the lowest considered coverage (1/4 and 1/2) the V atoms replace surface Pd atoms, and the oxygen atoms adsorb in a way which maximises their coordination to the V atoms. At 1 ML V and O coverage, the oxide forms a compact overlayer, with the most favourable stacking sequence being Pd(A)–Pd(B)–Pd(C)–V(B)–O(C). The local coordination of the V atoms at the interface is similar to that for bulk-V_2O_3 grown on Pd(1 1 1) and s-V_2O_3 (see Section 3.5). The results for the VO stoichimetry clearly confirm the trend towards V–Pd hetero-coordination already observed in the simulated annealing run, insofar, that at low oxidation numbers, the V atoms try to maximise their coordination to Pd atoms, preferentially, by replacing surface Pd atoms.

It is also important to stress that bulk VO is even less stable than the surface structures explored here so that the formation of a thick bulk VO phase on the Pd substrate is not possible. The calculated energies clearly show that, in the vicinity of a Pd surface, bulk VO will always decompose into V_2O_3 and V atoms forming a solid solution in Pd.

From these calculations, it is obvious that a further reduction of the vanadium oxide layer will always be accompanied by a tendency towards V–Pd hetero-coordination. The most stable model which we could determined for such films is characterised by three V atoms replacing Pd surface atoms and two oxygen atoms situated in those hollow sites which are surrounded by three V atoms (for details we refer to Ref. [6]). To explore further reduction we have considered adsorption of oxygen on a Pd-supported close-packed monolayer of V (models V_4O_1, V_4O_2 and V_4O_3), and a model in which three Pd surface atoms are replaced by V atoms and one O atom is placed in a hollow site (V_3O_1). In general, none of these structures are particularly stable, and, in all cases, a combination of V_2O_3 and vanadium in a bulk solution or the formation of a Pd–V surface alloy allows to lower the energy (see Fig. 6).

4. Discussion

4.1. Comparison with experiment

Comparison with experiment is somewhat hampered by the fact, that only limited microscopic data (STM) are yet available. To compare with experiment, we show the generalised surface energy versus the vanadium coverage for two different chemical potentials of oxygen, μ_O, in Fig. 7. In principle, the chemical potential can be related directly to the pressure of oxygen, p_{O_2}, but uncertainties are caused by density functional theory. The PW91 gradient approximation has the tendency to overestimate formation and binding energies [38,39] which means that the chemical potential might be shifted by several 100 meV. A change of the potential by 1 eV, corresponds to lowering the pressure by a factor of 10^{10} at 1000 K, and 10^{20} at 500 K (at least in the ideal gas regime). Using the theoretical binding energy of the oxygen molecule as reference, the upper limit for μ_O is 0, corresponding to oxygen molecules condensating on the surface (a pressure of course not accessible in the experiments). The potentials of -1.7 and -2.5 eV correspond to partial pressures of some 10^{-12} and 10^{-28} bar at $T = 500$ K [40,41], but again, the absolute pressures might be wrong by many orders of magnitude. We will therefore concentrate on the general trend and do not put a strong emphasis on the pressure scale.

The diagrams shown in Fig. 7 are easy to read (see also Section 2.2). Imagine that we want to determine the stability of oxide phases at 1 ML V coverage at a given chemical potential, μ_O. In the relevant diagram, only the energetically most favourable phases to the left and right of the 1 ML V line are stable. To guide the eye, the most stable phases are connected by lines. At $\mu = -1.7$ for instance, a mixture of s-V_2O_3 and r-VO_2 is expected to exist at 1 ML coverage. The diagram

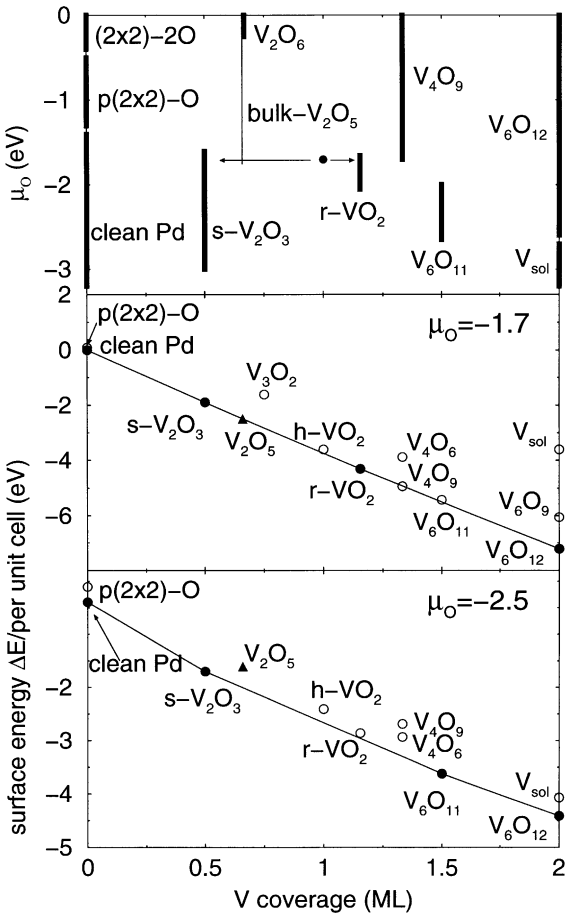

Fig. 7. Top panel: stable phases for varying oxygen potential and vanadium coverage. Two lower panels: change of the surface energy ΔE per (1×1) Pd(1 1 1) surface area upon adsorption of vanadium oxides for oxygen potentials $\mu_O = -1.7$, -2.5 eV (the energy zero for oxygen is defined by half the binding energy of the oxygen molecule). At a particular coverage the ordering of the labels agrees with the ordering of the phases at this composition. The energy change for adsorption of a single layer of bulk-V_2O_5 is shown as triangles. Table 2 describes the relevant phases.

also indicates that h-VO_2 is unstable under those conditions and decomposes into V_2O_3 and r-VO_2. The top panel indicates the stable phases as a function of the V-coverage and oxygen potential by black lines. At a given coverage and potential, the two phases to the left and right of the considered point are stable (as indicated by the black circle and the arrows in the graph).

At the $\mu_O = 0$, we find that only bulk-like V_2O_3 phases are thermodynamically stable at any coverage investigated here. The bulk-like V_2O_3 phases are oxygen terminated on both sides (V_2O_6, V_4O_9 and V_6O_{12}) and have no tendency to grow to thicker islands at low coverage and high oxygen pressures. Lowering the chemical potential of oxygen will make structures with high oxygen content less stable. In fact, at a potential of $\mu_O = -0.3$ eV, the oxygen richest phase, V_2O_6, becomes unstable, and thicker islands start to form even at lower coverage (V_4O_9). At a chemical potential of some $\mu_O = -1.3$ eV, chemisorbed oxygen on the Pd surface becomes unstable and oxygen evaporates from the Pd surface into the gas phase.

The first phase which is not related to bulk-V_2O_3 becomes stable at a potential of some -1.6 eV at low coverage (s-V_2O_3). At about the same potential ($\mu = -1.7$ eV), the rectangular VO_2 phase is stabilised, and V_4O_9 disappears. At $\mu_O = -2.2$ eV, the rectangular phase becomes unstable again, and a hexagonal VO_2 phase with s-V_2O_3 on top appears (V_6O_{11}). When we continue to lower the partial pressure further ($\mu_O = -2.65$ eV), the bulk like V_2O_3 phases (V_6O_{12}) are finally destabilised and vanadium starts to move subsurface. At a similar pressures ($\mu_O = -2.5$ eV), the hexagonal V_6O_{11} phase also starts to decompose, and the liberated V atoms go subsurface. Finally at about $\mu_O = -3.0$ eV, all oxides on the surface decompose, and the vanadium atoms disappear into the bulk.

How do our predictions compare to experiment. First it is clear that the phase diagram predicted by theory is complicated and astonishingly rich. Let us imagine, for instance, that we start from an oxygen rich phase at a nominal vanadium coverage of 1 ML and remove oxygen by slow heating (a similar preparation as used in Refs. [5,6]). At relevant pressures of a few mbar initially only bulk like V_2O_3 islands (V_4O_9) are stable. At $\mu_O = -1.6$ eV, a phase transition to a mixture of s-V_2O_3 and islands of bulk-V_2O_3 will occur. Decreasing the potential further to $\mu_O = -1.7$ eV will lead to s-V_2O_3 and patches of rectangular VO_2. Further decrease of the potential will destabilise the rectangular phase in favour of the hexagonal phase with s-V_2O_3 on top. This phase and s-V_2O_3 on Pd are stable over a wide pressure regime. At

$\mu = -2.6$eV, the 4(h-VO_2)/s-V_2O_3 (V_6O_{11}) phase decomposes and V diffuses into the bulk, with s-V_2O_3 wettening the whole Pd surface. With further reduction, finally all V atoms will move subsurface. These results agree very well with experiment, if we relate the rectangular VO_2 phase to the VO_2 phase observed in Ref. [5] (flower like pattern in LEED) and s-V_2O_3 to the VO termed phase of Ref. [5]. The last assignment was already shown to be correct in Ref. [6], but the assignment of the rectangular VO_2 phase to the "flower-phase" was only confirmed recently by STM and LEED [7].

One final note on bulk-V_2O_5 is appropriated here. We have included the stability of this phase in all diagrams of Fig. 7 (filled triangles and thin line in the top panel). At low V coverage and for oxygen potentials up to $\mu_O = -1.9$ eV, V_2O_5 is energetically stable. This confirms our previous assertion that kinetic instead of thermodynamic arguments must be responsible for the fact that V_2O_5 was not observed in the experiments. Possibly higher oxygen pressure can help to overcome the kinetic barriers involved in the formation of V_2O_5.

4.2. Surface stabilised models

In essence, our calculations predict three classes of stable thin films. At sufficiently high oxygen pressure or at sufficiently high V coverage, bulk-like V_2O_{3+x} phases are stable. These phases contain usually more oxygen than bulk V_2O_3, since both sides of the thin hexagonal slabs are oxygen terminated. This also implies that oxygen is located at the metal–oxide interface.

The second important category of films are the hexagonal and rectangular VO_2 films, which according to our calculations are only marginally less stable than bulk VO_2. Their bonding to the substrate is fairly week, and oxygen is again located at the metal–oxide interface. The origin of the stability of these films is difficult to disentangle, because the local coordination of the V atoms is mostly octahedral as in other films and bulk VO_2. Obviously the way the octahedra are linked in these structures (mainly edge sharing) is making them particularly favourable. The electronic density of states (DOS) of the r-VO_2 film is shown in Fig. 8. The lower peak located between -7 and -2.5 eV contains 6 electrons and is dominated by the oxygen 2p states (the O 2s states are at lower binding energies). At the Fermi-energy the V 3d states dominate. The minority V d band is unoccupied, and the majority band is occupied by 1 electron per V atom. Since the DOS is rather large at the Fermi-level, the film might well be a Mott–Hubbard insulator at low temperature.

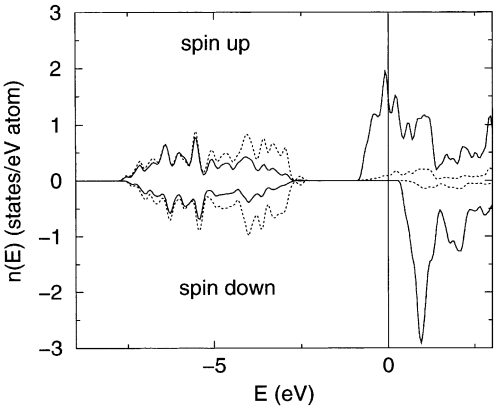

Fig. 8. Atom resolved electronic DOS for rectangular VO_2. The DOS on the V and O atoms are shown as full and dotted lines.

S-V_2O_3 is the third important structure, which is stable over a wide range of partial pressures at low V coverage. In this case, we find the V atoms in a trigonal coordination at the metal–oxide interface. There are some metastable phases (Pd/bulk-V_2O_3 – Fig. 3(a) and Pd/h-VO) which have a similar local V coordination, indicating that this coordination is particularly favourable for a V atom in contact with oxygen and the metal support. This is also confirmed by the layer resolved electronic density of states of s-V_2O_3 shown in Fig. 9. In a simple ionic picture the vanadium atoms donate three electrons to oxygen. But as can be seen in the layer resolved DOS the hybridization between O 2p and V 3d states is very strong (V d character at low binding energies). In a trigonal field, the five V-d bands split into three groups, two doubly degenerated E_g levels (d_{xy}, $d_{x^2-y^2}$ and d_{zx}, d_{zy} if the z-axis is orthogonal to the surface) and one A_g level ($d_{3z^2-r^2}$). All four E_g levels interact strongly with the oxygen p_z and one oxygen orbital in the xy-plane forming bonding and anti-bonding linear combinations. Also clearly visible is the hybridization

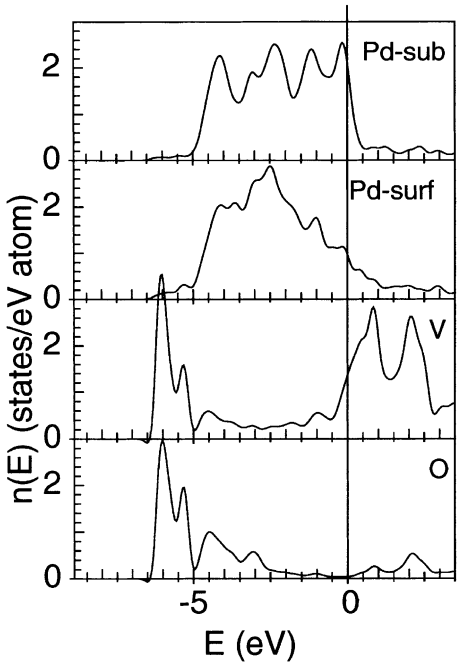

Fig. 9. Layer resolved electronic DOS for s-V_2O_3 on Pd(1 1 1). The DOS is shown for the Pd-subsurface layer (Pd-sub), the Pd-surface layer (Pd-surf), and the V atoms and O atoms. The lowest peak corresponds to the O 2p states.

between the V-d states and Pd-d states between -2 and 2 eV which leads to an additional upward shift of the V-d states and to a downward shift of the centre of the Pd states. The V–O and the V–Pd interactions combine in a way that opens a pseudo-gap at the Fermi level which is certainly an important factor for the stability of s-V_2O_3.

5. Conclusion

The results of our study are encouraging and demonstrate that the construction of (zero temperature) phase diagrams for binary compounds on a support is possible by means of first-principles calculations. This might actually have far fetched consequences, for instance, in heterogenous catalysis, where structural model are nowadays often based on microscopic ultra high vacuum measurements, such as STM, and/or first-principles modelling corresponding to such conditions. By including the oxygen pressure and the metal coverage much of these deficiencies can be removed, and we hope that our work will encourage similar studies in the future.

The "example" system considered here is complex and interesting on its own. To date similar studies have only been performed for the surfaces of binary systems, where only one extensive thermodynamic variable needs to be considered [20–23]. Our study is also significantly complicated by the fact that vanadium occurs in four oxidation states so that one is forced to consider varying stoichiometries. Given all these obstacles, it is remarkable how well our predictions agree with experiment: At high oxygen pressure, mostly bulk-like V_2O_{3+x} phases are stable. These films contain more oxygen than bulk V_2O_3, since both sides of the thin hexagonal slabs are oxygen terminated. When the pressure is decreased, a surface mediated (2×2) V_2O_3 phase is stabilised and remains stable over a wide range of physical parameters. A rectangular and a hexagonal VO_2 phase are expected to grow in the same pressure regime as s-V_2O_3 but at somewhat higher V coverage. These thin films differ completely in terms of structure and geometry from bulk VO_2. In fact, the models were obtained by cleaving and relaxing vanadium-*monoxide* along (1 1 0) or (1 1 1) planes leaving the local coordination of vanadium atoms unchanged. The lattice parameters of the novel rectangular oxide phase seem to agree with the structural parameters of the experimentally observed "flower" phase [5]. Recent experimental STM work confirms this conjecture [7]. If the partial oxygen pressure is further reduced, all phases finally decompose and V is supposed to migrate into the Pd bulk, which fully agrees with the experimental data available [5].

Finally, it seems important to highlight the procedures we have adopted in the construction of thin layers grown on a metal support. The first step was a careful investigation of bulk phases. From this study we learned how the basic building units (in our case VO_6 octahedra) can be assembled to build favourable oxides. In a second step, unsupported thin layers were investigated. They usually constitute a good starting guess for compact densely packed oxide over-layers on the metal support. The study of thin unsupported layers was

supplemented by simulated annealing runs performed at rather low vanadium and oxygen coverage. The insight gained from these calculations was then used to construct thin supported layers at varying coverage and stoichiometry. Similar procedures should prove helpful for a wide variety of thin oxide films and metal–oxide interfaces.

Acknowledgements

This work was supported by the Austrian Science Funds within the Joint Research Project on "Gas–Surface Interaction" grant no. S8106-PHY.

References

[1] V.E. Henrich, P.A. Cox, The Surface Science of Metal Oxides, Cambridge University Press, Cambridge, 1993.
[2] R. Franchy, Surf. Sci. Rep. 38 (2000) 195.
[3] S. Chambers, Surf. Sci. Rep. 39 (2000) 105.
[4] C. Noguera, J. Phys.: Condens. Matter. 12 (2000) B367.
[5] F.P. Leisenberger, S. Surnev, L. Vitali, M.G. Ramsey, F.P. Netzer, J. Vac. Sci. Technol. A 17 (1999) 1743.
[6] S. Surnev, L. Vitali, M.G. Ramsey, F.P. Netzer, G. Kresse, J. Hafner, Phys. Rev. B 61 (2000) 13945–13954.
[7] S. Surnev, G. Kresse, M.G. Ramsey, F.P. Netzer, Phys. Rev. Lett. 87 (2001) 086102.
[8] M. Sock, S. Surnev, M.G. Ramsey, F.P. Netzer, Topics Catal. (2000) in press.
[9] W. Kohn, L. Sham, Phys. Rev. 140 (1965) A1133.
[10] R.O. Jones, O. Gunnarsson, Rev. Mod. Phys. 61 (1989) 689.
[11] R. Car, M. Parrinello, Phys. Rev. Lett. 55 (1985) 2471.
[12] M.C. Payne, M.P. Teter, D.C. Allan, T.A. Arias, J.D. Joannopoulos, Rev. Mod. Phys. 64 (1992) 1045.
[13] G. Kresse, J. Hafner, Phys. Rev. B 48 (1993) 13115.
[14] G. Kresse, J. Furthmüller, Comput. Mater. Sci. 6 (1996) 15.
[15] G. Kresse, J. Furthmüller, Phys. Rev. B 54 (1996) 11169.
[16] P.E. Blöchl, Phys. Rev. B 50 (1994) 17953.
[17] G. Kresse, D. Joubert, Phys. Rev. B 59 (1999) 1758.
[18] Y. Wang, J.P. Perdew, Phys. Rev. B 44 (1991) 13298.
[19] J.P. Perdew, J.A. Chevary, S.H. Vosko, K.A. Jackson, M.R. Pederson, D.J. Singh, C. Fiolhais, Phys. Rev. B 46 (1992) 6671.
[20] X.-G. Wang, W. Weiss, S.K. Shaikhutdinov, M. Ritter, M. Petersen, F. Wagner, R. Schlögl, M. Scheffler, Phys. Rev. Lett. 81 (1998) 1038.
[21] P. Raybaud, J. Hafner, G. Kresse, S. Kasztelan, H. Toulhoat, J. Catal. 189 (2000) 129–146.
[22] P. Raybaud, J. Hafner, G. Kresse, S. Kasztelan, H. Toulhoat, J. Catal. 190 (2000) 128–143.
[23] X.-G. Wang, A. Chake, M. Scheffler, Phys. Rev. Lett. 84 (2000) 3650.
[24] G. Kresse, in press.
[25] E. Enjalbert, J. Galy, Acta Cryst. C 42 (1986) 1467.
[26] A. Chakrabarti, K. Hermann, R. Druzinic, M. Witko, F. Wagner, M. Petersen, Phys. Rev. B 59 (1999) 10583–10590.
[27] K. Hermann, A. Chakrabarti, R. Druzinic, M. Witko, Phys. Stat. Sol. (a) 173 (1999) 195.
[28] D. Taylor, Trans. J. Brit. Cermic Soc. 83 (1984) 32.
[29] P.D. Dernier, J. Phys. Chem. Solids 31 (1970) 2569.
[30] N.F. Mott, Metal–Insulator Transitions, Taylor and Francis, London, 1990.
[31] L.F. Mattheiss, J. Phys.: Condens. Matter. 8 (1996) 5987.
[32] M. Catti, G. Sandrone, R. Dovesi, Phys. Rev. B 55 (1997) 16122.
[33] S.Yu. Ezhov, V.I. Anisimov, D.I. Khomskii, G.A. Sawatzky, Phys. Rev. Lett. 83 (1999) 4136.
[34] S. Kumarakrishnan, N.L. Peterson, T.O. Mason, J. Physics, Chem. Soilds 46 (1985) 1007.
[35] E. Wimmer, K. Schwarz, R. Podloucky, P. Herzig, A. Neckel, J. Phys. Chem. Solids 43 (1982) 439.
[36] Ch. Konvicka, Y. Jeanvoine, E. Lundgren, G. Kresse, M. Schmid, J. Hafner, P. Varga, Surf. Sci. 463 (2000) 199.
[37] D.R. Jennison, C. Verdozzi, P.A. Schultz, M.P. Sears, Phys. Rev. B 59 (1999) R15605.
[38] S. Kurth, J.-P. Perdew, P. Blaha, Int. J. Quantum Chem.75 (1999) 889.
[39] B. Hammer, L.B. Hansen, J.K. Nørskov, Phys. Rev. B 59 (1999) 7413.
[40] S. Bhattacharjee, The expert system for thermodynamics, http://eng.sdsu.edu/testcenter/index.html.
[41] D.R. Stull, H. Prophet, JANAF Thermodynamical Tables, US National Bureau of Standards, Washington, DC, 1971.